



HAL
open science

Sizing a hybrid hydrogen production plant including life cycle assessment indicators by combining NSGA-III and principal component analysis (PCA)

Hemant Sharma, Guillaume Mandil, Élise Monnier, Emmanuelle Cor, Peggy Zwolinski

► To cite this version:

Hemant Sharma, Guillaume Mandil, Élise Monnier, Emmanuelle Cor, Peggy Zwolinski. Sizing a hybrid hydrogen production plant including life cycle assessment indicators by combining NSGA-III and principal component analysis (PCA). *Energy Conversion and Management*: X, 2023, 18, pp.100361. 10.1016/j.ecmx.2023.100361 . hal-03993455

HAL Id: hal-03993455

<https://inria.hal.science/hal-03993455v1>

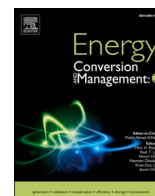
Submitted on 7 Aug 2024

HAL is a multi-disciplinary open access archive for the deposit and dissemination of scientific research documents, whether they are published or not. The documents may come from teaching and research institutions in France or abroad, or from public or private research centers.

L'archive ouverte pluridisciplinaire **HAL**, est destinée au dépôt et à la diffusion de documents scientifiques de niveau recherche, publiés ou non, émanant des établissements d'enseignement et de recherche français ou étrangers, des laboratoires publics ou privés.



Distributed under a Creative Commons Attribution 4.0 International License



Sizing a hybrid hydrogen production plant including life cycle assessment indicators by combining NSGA-III and principal component analysis (PCA)

Hemant Sharma^{a,b,*}, Guillaume Mandil^c, Élise Monnier^a, Emmanuelle Cor^a, Peggy Zwolinski^b

^a Université Grenoble Alpes, CEA-Liten, 17 rue des Martyrs, F-38054 Grenoble, France

^b Université Grenoble Alpes, G-SCOP laboratory, 46 av. Félix Viallet, Grenoble 38031 cedex 1, France

^c Université Grenoble Alpes, CNRS, INRIA, Grenoble INP, LJK, 38000 Grenoble, France

ARTICLE INFO

Keywords:

Many-objective optimization
NSGA-III
Objective reduction
Life Cycle Assessment
Energy systems

ABSTRACT

In the design and synthesis of energy systems, mathematical tools such as optimization algorithms are often used. While using them, environmental indicators are increasingly used as optimization criteria to exploit the possible environmental benefits of these systems. The problem is that the high number of environmental indicators poses a problem for optimization algorithms in terms of convergence, computational time and visualization. In this paper, this problem is addressed through a many-objective search of solutions using a state-of-the-art evolutionary algorithm, NSGA-III. Furthermore, the performance of this algorithm is tested using different settings in the PCA-based objective reduction framework. The original 14 indicators are reduced to seven, four, three and two, which reveal important insights about the use of NSGA-III, objective reduction and a combination of the two. It was found that by using objective reduction, the performance of NSGA-III can be further improved in terms of the quality of solutions and computational time. However, beyond a certain point, further objective reduction leads to a trade-off between solution quality and computational time. For this case study, the best quality solutions were obtained in the PCA reduction procedure when the CUT value was maintained at 99.99% without additional reduction in the last step, using a correlation matrix. The algorithms were applied to a real-life sizing case study involving hydrogen production from polymer-electrolyte-membrane (PEM) water electrolysis, for which the demand is furnished by the electricity spot market, solar photovoltaics (PV) or wind turbine in Marseille, France. These results will be useful for future applications of many-objective optimization and objective reduction. They will also be practical for including environmental indicators in the many-objective search for solutions.

1. Introduction

1.1. Background and motivation

Due to the urgency regarding ever-increasing environmental impacts, it is necessary to take that into account while designing our systems. Thus, while using optimization algorithms, it is also necessary to include environmental indicators as optimization objectives, so that the environmental benefits of systems are sufficiently exploited. This becomes especially relevant for energy systems, owing to their large contribution to global warming impact [1]. It also becomes important that the impact transfer is curbed as much as possible while designing new energy systems.

While designing energy systems in the literature, the environmental criteria are often left out. Falahi et al. reviewed optimization methods in

solar and wind-based hybrid energy systems [2]. They found that environmental criteria were considered only in a quarter of reviewed studies. Sharma *et al.* also report that environmental criteria are insufficiently included in the commercially available hybrid energy design software [3].

Life Cycle Assessment (LCA) is commonly used to assess the environmental performance of energy technologies [4]. It takes into account all the materials, processes and environmental exchanges taking place during the complete lifetime of a product. The environmental impact of products is then calculated regarding different indicators, such as global warming potential, acidification, eutrophication, etc. This methodology thus ensures a fair comparison between different products satisfying the same function while avoiding impact transfer to another life cycle phase or indicator.

* Corresponding author.

1.2. Optimization studies that include LCA indicators

The number of optimization studies that include LCA indicators as objectives are gradually increasing. Owing to the added complexities with higher objectives in optimization, only a limited number of LCA indicators are typically included.

The earliest examples of LCA indicators in optimization are found in the late 1990s when Azapagic et al. used the E-constraint method to simultaneously optimize production, cost, and global warming potential to manage a chemical process chain [5]. Zhang et al. also used the same method to assess various system configurations in microgrids [6]. They included global warming potential and acidification potential as two environmental indicators. Yue et al. proposed a hybrid LCA/many-optimization framework to include greenhouse gas emissions in the decision-making of biomass supply chains in the UK [7]. Antipova et al. included six environmental indicators with other conventionally used indicators, such as cost, to investigate alternatives for the retrofitting of buildings [8]. More recently, van de Paer et al. included three LCA indicators, along with cost, to investigate future energy scenarios in Switzerland [9].

Evolutionary algorithms (EA) have also been used to include LCA indicators as optimization objectives. Gerber et al. used a genetic algorithm in the process design of a biomass plant that utilizes wood chips to generate synthetic natural gas and heat/electricity [10]. They used thermodynamic design as the technical constraint, and cost and Eco-Indicator 99 as an aggregated environmental indicator to search for acceptable solutions. Ahmadi et al. used NSGA-II, a Pareto-based genetic algorithm for the eco-design of a conventional water production process [11]. Three objectives were included in the main optimization loop for this purpose: water quality indicator, cost, and an aggregated environmental score. The design of hybrid energy systems, similar to the ones in this paper, was done by Nagarpurkar et al. using genetic algorithms [12]. They included CO₂ emissions with the techno-economic design of microgrids in the United States. Luo et al. optimized the operation strategy of distributed energy systems using NSGA-II. They included CO₂ emissions as an objective [13]. The sizing and operation of pharmaceutical batch plants were optimized by Dietz et al. while using genetic algorithms [14]. They included aggregated environmental impact and cost as the optimization criteria.

1.3. The problem with including LCA indicators as optimization objectives

It was seen that although LCA indicators have been included in optimization studies, only a limited number of them are usually included. It is important to include most of them to avoid impact transfer. It could be argued that these indicators could be aggregated into a single environmental indicator, or endpoint indicators could be used instead. When the former is done, there is a risk of ruling out solutions that are optimal in the original objective space. Since the objectives disproportionately contribute to the final impact, the dominance structure of the original problem is distorted. This was demonstrated by Antipova et al.: they found that using the total Eco-Indicator 99 alone favored only one group of indicators [15]. It resulted in the optimization algorithm omitting one set of otherwise optimal solutions.

On the other hand, the LCA indicators are numerous, and they are increasing with every update. For instance, the recently updated impact assessment methods ReCiPe2016 and IMPACT World + have more than 15 midpoint indicators [16,17]. This poses convergence problems for optimization algorithms.

1.4. NSGA-III as an optimization algorithm

Along with EA, there has been an increased interest in Particle Swarm Optimization (PSO). Baghaee et al. used multi-objective PSO to size a micro-grid system including wind, PV, electrolyzer, fuel cells, and

hydrogen storage [18]. PSO is claimed to be easier to implement than EA but it is complex to visualize and represent when dealing with 3 + optimization parameters [19]. The performance comparison between the two techniques is found to be problem dependent in the literature. Hassan et al. concluded that PSO outperforms EA in computational efficiency for nonlinear problems. The comparative performance was better for PSO when nonlinear problems were unconstrained with continuous design variables [20]. Whereas, other studies observed that EA performed better than PSO in terms of the computational time and convergence [21,2].

In this paper, we use EA for many-objective optimization. They are relatively robust and can handle a variety of different problem types: non-linear, continuous/discrete, and even black-box models [22]. Another advantage is that its computations can be run in parallel, thus multiple computers can be deployed to solve a large problem.

Amongst them, NSGA-III is one of the state-of-the-art evolutionary algorithms for many-objective optimization [23]. It was first introduced in 2014 in response to the convergence problems mentioned in the previous subsection [24]. Its performance in terms of convergence and diversity for up to 15 objectives was also demonstrated [25]. Another key advantage of this algorithm is the preferential search of the Pareto front. Due to its reference-points-based approach, it inherently searches for preferred points. It becomes convenient with a high number of objectives since the size of the Pareto front becomes large and not all parts could be of interest. As a result, post-Pareto processing to select particular solutions for decision-making might not be necessary.

1.5. Objective reduction techniques to improve performance

The life cycle impact indicators are observed to be highly correlated in the literature [26,27]. Even though NSGA-III seems like a sound algorithm to deal with a high number of objectives in optimization, its performance in terms of convergence and calculation time could be further improved by leveraging the correlations. This is called 'objective reduction' in the literature [28]. Objective reduction techniques indeed improve the performance of various evolutionary algorithms in terms of lower computational time and better quality results in the literature [29–32]. Additionally, the visualization of a high number of indicators can be substantially improved using correlations between them.

1.6. Content and contribution to the literature

An important contribution of this paper is obtaining insights into the influence of objective reduction procedures on many-objective optimization. It was found that objective reduction indeed improved both: the optimization time required and the quality of solutions obtained. However, objective reduction beyond a certain point might distort the structure of the original Pareto front. It thus informs about the trade-off between computational time and solution quality. It also warns against arbitrary reduction in indicators using pre-defined settings, as a small amount of variance left out might have a large influence on the Pareto front.

For obtaining the above conclusions, the PCA objective reduction procedure is tested with different settings. The original 14 indicators are reduced to two, three, four, and seven indicators. It was found that, for this case study, when reducing indicators to seven, there were improvements in computational time, convergence, and diversity of solutions. The seven indicators corresponded with the following setting in the PCA reduction framework of Saxena et al.: threshold value (CUT) of 99.99% and skipping the last step of additional reduction of indicators [33]. Where CUT is the cumulative contribution of the retained principal components for indicator reduction. Other settings reduced the indicators to less than seven which improved the computational time but reduced the quality of the solutions obtained.

Another contribution of this paper is that the objective reduction techniques are combined with NSGA-III. To the best of our knowledge,

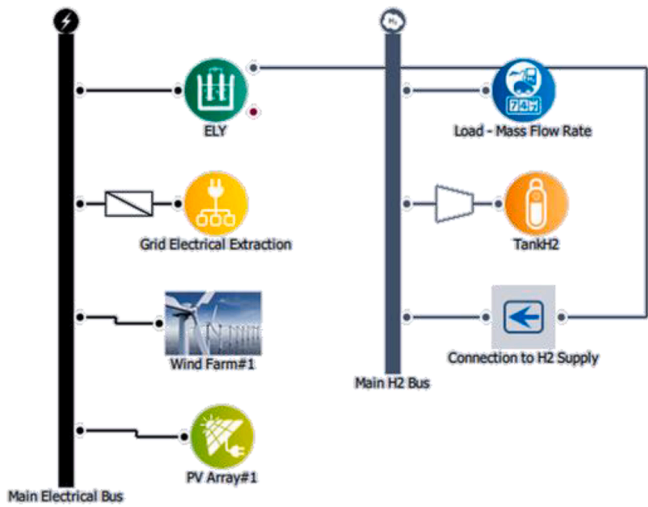


Fig. 1. Representation of the case study in Odyssey.

this has not been done and, consequently, its performance with or without objective reduction was unknown. Even though the preliminary estimates and the literature point in a positive direction, the performance needs to be verified and quantified. In this paper, the performance of NSGA-III is thus tested with and without leveraging the correlations on a sizing problem of a hydrogen production plant. This real-life case study involves PEM electrolyzers, for which the demand is furnished by the electricity grid, solar PV, or wind turbine in Marseille, France.

Thus, the case study is described in the following section. Then, in the third section, algorithms, the objective reduction technique, and the research approach is described. Results are outlined in Section four, followed by discussions and conclusions.

2. Problem description

2.1. Overview

This section describes the overall function of fitness evaluation. As described above, the case study is the sizing of a plant producing hydrogen using (PEM) electrolysis of water in Marseille, France. The electricity is supplied by the grid, photovoltaics, and/or wind turbine. The aim is to determine the size of each technological component while taking into account the technical, economic, and environmental indicators. Fitness is thus evaluated in terms of these indicators. The design variables are, therefore, the sizes of solar PV, wind turbine, PEM electrolyzer, and the number of hydrogen storage tanks.

2.2. Fitness function

The fitness for the technical and economic indicators is evaluated using the hybrid energy simulation software, Odyssey. Whereas the fitness for environmental indicators is evaluated by LCA methodology using Brightway2[34]. The Odyssey software is developed by the French Commission of Atomic and Alternative Energies [35]. It can be used to optimize system design and energy management. It has high-precision models for each technology and calculates the operation of each component for each time step, for one year. This then enables the estimation of the techno-economic indicators for the project lifetime. The operation details and energy flows of each component are imported to Python and used to calculate LCA indicators using Brightway2 [34]. The case study as visualized in the Odyssey software can be seen in Fig. 1 and the computational structure with NSGA-III can be seen in Fig. 2.

2.3. Fitness or performance indicators

The indicators to quantify fitness or system performance are discussed in this paragraph. These indicators are also the optimization objectives in this paper. The technical indicator is the unsatisfied hydrogen demand, which can be expressed as the percentage of the total mass-based hydrogen demand that the system was unable to satisfy during the project’s lifetime. The economic indicator is the levelised cost (€) per kg of hydrogen. For LCA, 13 midpoint indicators from IMPACT World + are selected [17]. These are outlined in Table S1 in supplementary material along with their abbreviations. The main reason for this selection was that they were recently updated according to the developments in the impact pathways.

2.4. Constraints or Operating rules

Grid electricity is used if the electricity price is less than 50 €/MWh. The electrolyzer is operated at maximum power during this time. However, if local sources of PV or wind are available, subject to local conditions, the use of their electricity is preferable. Thus, there are 4-time series that vary in steps of five minutes for one year: hydrogen demand, grid electricity price, wind power production, and PV power production. To account for the potential mismatch between hydrogen production and demand, storage tanks are included as well.

2.5. Inputs to the integrated model

The model or the fitness function is further described in this subsection in terms of the inputs and data sources. The economic inputs are for the demonstration of the approach only, and they are based on the default values found in the literature. Project lifetime is assumed to be 20 years as it is the often-used value for similar energy projects. A summary of the model inputs is presented in Table S2 in supplementary

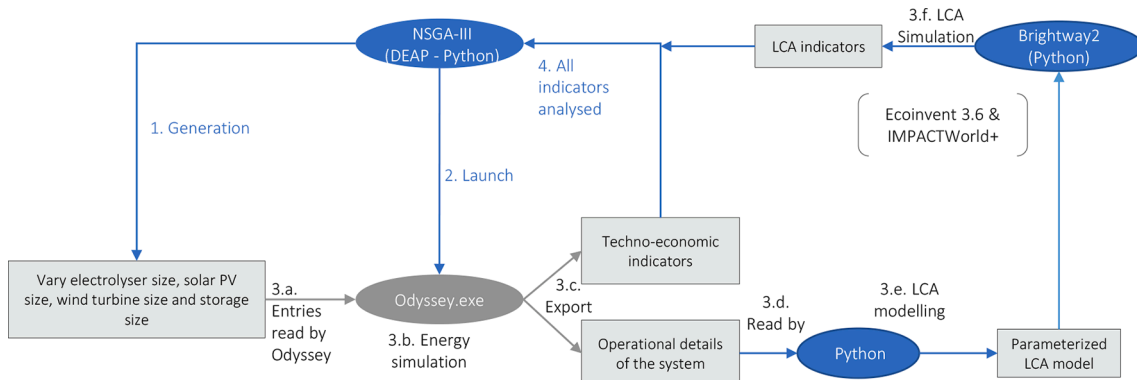


Fig. 2. Computational structure for the search of solutions including technical, economic, and LCA indicators.

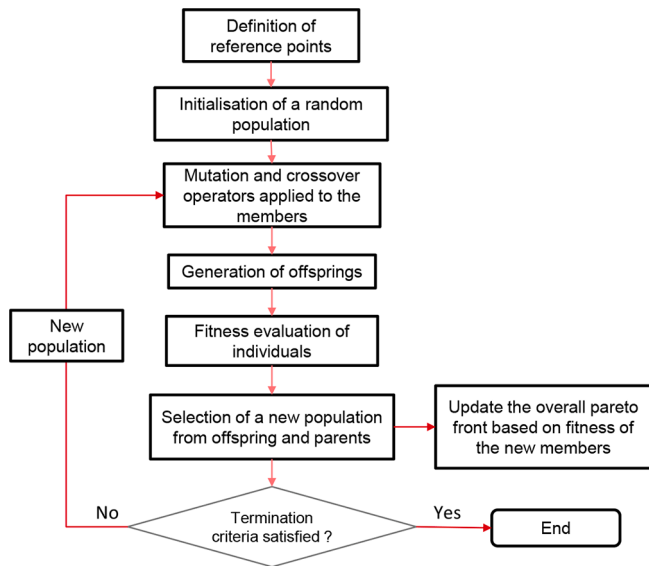


Fig. 3. The NSGA-III operating scheme in this paper.

material and is also described below:

2.5.1. Electrolyser

data can be seen in Tables S3 and S4 in supplementary material, which is based mainly on the literature [36,37]. The stack lifetime is assumed to be 90,000 h.

2.5.2. Solar PV

production data is taken from the freely available database renewable.ninja [38]. For the location of Marseille, France, the capacity factor is 0.19. The LCA model for solar PV is taken from the database Ecoinvent v3.6 for multi-Si technology, updated according to more recent industrial data [39].

2.5.3. Wind

production data is taken from renewable.ninja also [40]. The LCA inventory is from the literature and is available online [41,42] for adaptation as a Python notebook. It is a parameterized model that calculates a detailed inventory using a limited amount of parameters such as turbine size, type (offshore or onshore), etc.

2.5.4. Hydrogen storage tanks

are operated within a range of 30–60 bar. Pressure cannot be dropped below 30 due to technical constraints. The environmental impact of storage was not included since the goal of the case study was a demonstration of a global approach rather than a calculation of the exact environmental impact. Ideally, it should indeed be included.

2.5.5. Other LCA inputs

The LCA boundary selected is cradle to grave. It includes as many impacts as possible throughout the project’s lifetime, including raw material extraction, fabrication of components, use phase, and transport until end-of-life. For transport, the default values used in the market mixes are used.

The geographical preference for all activities is selected in terms of increasing the geographical area around France (e.g. France, neighboring countries, Europe, Global). These preferences are coded in Brightway2 to select the activities in Ecoinvent v3.6 closest to the desired geographical scope.

For end-of-life, only the recycling of materials for which the activities are available in Ecoinvent v3.6 (metals and plastics) are included [43]. The system is credited for recycling by avoiding the production of virgin materials. The recycling rate is set at 50% and the rest of the materials are either landfilled or incinerated.

3. Materials and methods

3.1. Genetic algorithm: NSGA-III

A simplified illustration of the algorithm is provided in Fig. 3. It is briefly described in this subsection using the original paper [24] and its implementation in this paper using the DEAP framework in Python [44].

The first step is the specification of reference points which essentially dictates the preferred Pareto points to be searched. Reference points in NSGA-III are specified in terms of the objectives either as a uniform spread or as a set of preferential points. These points lie between 0 and 1, representing the minimum and maximum value of each objective respectively.

If a uniform spread of reference points is desired, an approach from Das et al. is proposed by the authors of NSGA-III [45]. It involves placing points on a normalized hyperplane with an intercept = 1 on each axis. The number of points (H) is calculated as

$$H = \frac{(N_{OBJ} + \hat{P} - 1)!}{\hat{P}! \times (N_{OBJ} - 1)!} \tag{1}$$

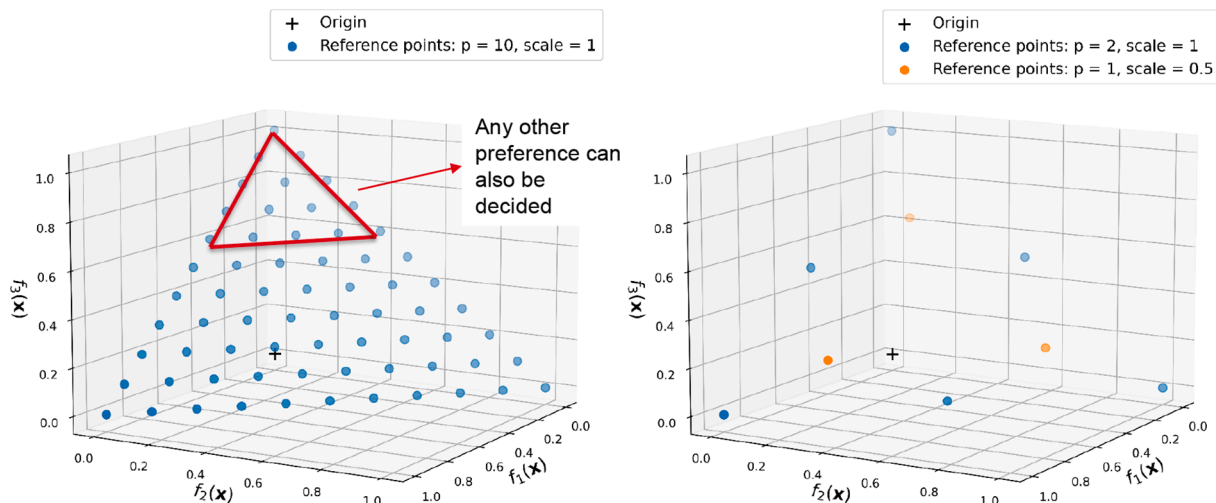


Fig. 4. Reference point distribution illustrated for three dimensions. (Left) For 10-axis partitions. (Right) Using a layering approach when the number of objectives increases.

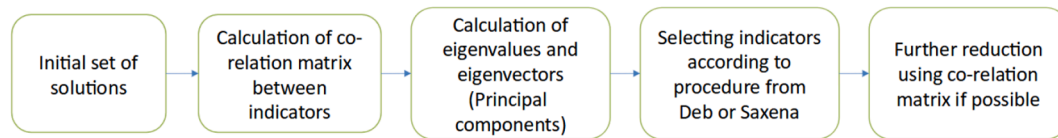


Fig. 5. An illustration of the methodology to select indicators using PCA heuristics as proposed in the literature [31,33].

where, \hat{P} is the number of axis partitions and N_{OBJ} is the number of objectives. For example, for three objectives with 10 axis partitions, 66 reference points are obtained, shown on the left in Fig. 4. Any other preferential set of points can also be decided instead.

These reference points increase exponentially with the number of objectives. For instance, when the number of objectives is increased to 10, the number of reference points becomes 92,378. To keep this in check, the authors propose decreasing the number of axis partitions but using multiple layers at different scales. For example, on the right in the same Figure, the layering approach in three dimensions is shown when the objectives increase.

Then, a pseudo-random population is initialized, meaning random individuals (system configurations) within the search range. For example, for a solar PV size range of 0–8 MW, random sizes between this range are generated for the individuals in the first generation. Often the population size is slightly higher than the number of reference points. Offsprings from the parent population are produced by applying crossover and mutation operators. The fitness or performance indicators of each individual in the two populations are then evaluated.

Then, the next generation is selected from the parents and offspring. This step is probably the most complex part of the algorithm. With the increase in objectives, the number of non-dominated solutions increases exponentially. In NSGA-III, individuals are first sorted into levels of non-domination. In simple terms, the non-dominated solutions are filled first, then the algorithm goes to the second-best level until the number of selected members is equal to or more than the population size. If the size of the population is equal to the number of individuals in the selected levels, no further steps are required, and the next generation can be started.

However, often this is not the case, especially when the number of objectives increases and a large number of individuals become non-dominated. Selection is to be made amongst individuals at a particular non-domination level such that the population size remains constant throughout the evolutionary process. For this, individuals are differentiated according to their diversity, using the reference points. All other individuals in the higher domination levels are discarded. The algorithm then proceeds to the next step and so on until the termination criterion is satisfied. The selection step ensures that well-converged and diverse solutions are obtained. This is also the stage where the previous generation algorithms, NSGA-II and SPEA2, struggled.

The Pareto front is updated at each generation from the population by retaining only the non-dominated members. The population size remains constant, but the number of Pareto front members usually increases with generations.

3.2. Objective reduction using principal component analysis (PCA)

PCA is one of the techniques often utilized in the literature for objective reduction. It is a statistical tool that is used for the analysis of complex data, or more specifically, the identification of redundant variables that do not add new information but complicate the data. It allows the transformation of co-related variables into a set of ordered, uncorrelated variables, known as principal components (PCs). PCs can be ranked according to their ability to explain the variance in the data set [31]. In many practical problems, only a few PCs explain most of the variance in the entire set. In the context of LCA, each PC is a combination of original impact indicators. Once the PCs explaining the maximum

variance are identified, indicators making the maximum contribution in them can be selected.

The following are the steps to reduce the number of objectives, as per the authors [31,33], outlined in Fig. 5. The first step is the calculation of a correlation matrix of the LCA indicators. As the name suggests, it contains correlation coefficients between every combination of indicators. Eigenvectors and eigenvalues of the matrix are then calculated. The first PC is then the eigenvector corresponding to the highest eigenvalue. The second PC is the eigenvector with the second highest eigenvalue and so on. Next, only the PCs which explain the maximum variance are retained. As mentioned previously, the threshold cut value to retain the principal components is pre-defined (CUT). When the cumulative explained variance of the retained principal components exceeds the CUT value, additional PCs are not analyzed. Generally, the recommended value is 99.7%, but for problems with a high number of redundant indicators, Saxena et al. demonstrated that even values as low as $\approx 68\%$ could be used to explain most of the variance in the original objectives [33].

Impact indicators in the retained PCs are then selected according to two rules as per Saxena et al. [33]:

1. Objectives with the most negative and most positive values are chosen
2. If all objectives have the same sign, two objectives with the highest values are chosen

Then, in the final step, the selected indicators are further reduced according to the correlation coefficients between them. For this step, Saxena et al. introduced quantifiable parameters to facilitate this step such as a correlation threshold and a selection score [33].

3.2.1. PCA settings for optimization

To apply the above-described procedure in this paper, the optimization is run for five generations to obtain a sample set. Then, two settings in the procedure are varied: the threshold value of retaining principal components (CUT) and the last step of reducing additional indicators using a correlation matrix. This was done to find the influence of these two settings on the final results. Changing the two above steps changes the number and the type of indicators retained for the optimization. Based on them, insights about these settings for future use could be obtained.

In the *first instance*, the CUT value is maintained at 99.99% and all the steps in Fig. 5 are followed. This resulted in the selection of two indicators even when the procedure was repeated three times: *freshwater ecotoxicity* and *ionizing radiations*. This was only repeated three times since the quality of solutions obtained was significantly worse for this instance.

In the *second instance*, the CUT value is decreased to 95% without additional reduction using a correlation matrix. This allows for retaining more indicators since poor quality of solutions for the *first instance*. This value was also used in the other investigations in the literature [32,46] according to the first proposal of the PCA reduction framework [31]. This resulted in the retention of three to four indicators.

In the *third instance*, gaining experience from the results, the CUT value is maintained at 99.99% without any further correlation-based reductions. A summary of the retained indicators for all simulation runs can be seen in Table 1. An elaboration of the reduction procedure using sample calculation for the first and second instances can be found

Table 1
Reference points, population size, and indicators retained for the different simulation runs.

instance	Original objectives	CUT = 99.99% (1 st instance)	CUT = 95% without additional reduction of indicators (2 nd instance)	CUT = 99.99% without additional reduction of indicators (3 rd instance)
No. of objectives (N_{OBJ})	14	2	4	7
Axis partitions (\hat{P})	2,2	72	6	11
Layer scale	1,0.5	1	1	1,0.5
No. of reference points (H)	210	73	84	112
Population size	212	80	92	120
Indicators for search	Cost, FS, W, IO, Oz, CC, Min, FWA, TER, PM, POF, HT non can, HT can, FW eco	IO, Fw eco	IO, HT can, POF, W/CC	IO, W, HT can
No. of simulation runs	5	3	5	5

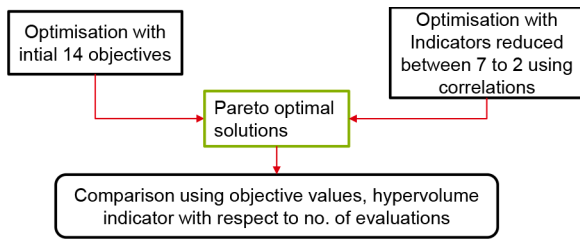


Fig. 6. A comparison scheme for testing the performance of different optimization cases .

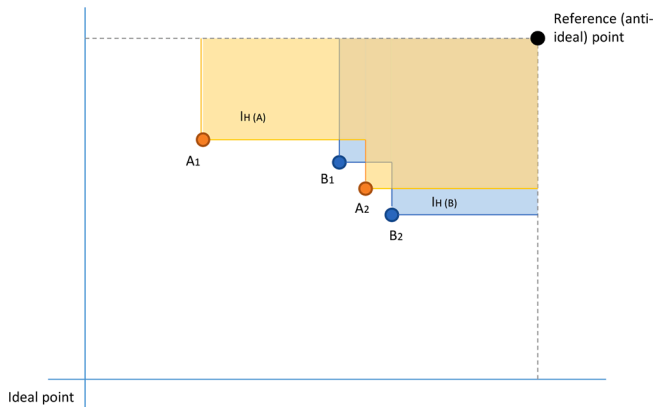


Fig. 7. The hypervolume calculation principle [50].

in [Section 1 in the supplementary material.](#)

3.3. Comparing the algorithms

As previously mentioned, the performance of NSGA-III is compared with and without the indicator reduction techniques. Thus, the original set of indicators is 14, and they were reduced to between two to seven as seen above. The performance of the algorithms is then estimated by comparing the quality of the Pareto front in terms of convergence and diversity, using a hypervolume indicator. Furthermore, the minimum objective values are also recorded for the number of evaluations. A comparison schematic can be seen in [Fig. 6.](#)

3.3.1. Hypervolume indicator

Hypervolume indicator is widely used to measure the quality of solutions proposed by many-objective optimization in terms of their convergence and diversity [47]. The former means its closeness to the optimal set, while the latter means the spread of solutions in the entire

objective space [48]. It quantifies this by measuring one single value: the portion of space in all objectives covered by a set of solutions. The space is measured with respect to a non-ideal point. This point is generally between 5–50% worse than the worst point expected in the set [49]. Hypervolume indicator is especially useful in practical problems when the exact Pareto front is not known.

For example, consider two solution sets with two points each: A and B. [Fig. 7](#) shows the space covered by the respective solution sets in the two objective spaces if the goal is to minimize the two objectives f_1 and f_2 . As the solutions become widely distributed (diversity) or closer to the ideal point (convergence), the space covered by them increases. The hypervolume calculation algorithm proposed by While et al., available online, is used in this paper [48].

3.3.2. Definition of reference points

Reference point, and consequently population size selection, is important for analyzing the performance of the three instances since it will directly influence the number of function evaluations for each generation and thus the time required for each simulation run. As seen in [Eq. 1](#), since the number of objectives (N_{OBJ}) are fixed, axis partitions (\hat{P}) are needed for defining the number of uniformly distributed reference points. The higher the number of partitions, the better it is, since more diverse solutions for each objective can be obtained. This number then decides the number of reference points and consequently the population size. Following the authors, the population size is slightly higher than the reference points [24].

The population size is also important since it should be large enough to ensure that sufficiently different individuals are present in generation zero. Thus, firstly a minimum population size is decided to be 80.

For two objectives, 72 axis partitions result only in 73 reference points and minimum population size. Then, for three objectives, 11 axis partitions can be afforded which results in 78 reference points. The axis partitions are reduced for four objectives to get 84 reference points. From seven objectives onwards, layering is needed since even with $\hat{P}=5$, H becomes 462. Thus, for two layers, one outer layer with three-axis partitions and a second inner layer with two-axis partitions are selected. For 14 objectives, \hat{P} for the outer layer has to be reduced to two; otherwise $H = 665$. It cannot be reduced further since, as seen in [Fig. 4](#), for $\hat{P}=1$ only the extreme points of each objective are selected. An overview of the different instances is provided in [Table 1.](#)

4. Results

4.1. Hypervolume indicator

The hypervolume indicator value for optimization runs with different numbers of reduced objectives is shown in [Fig. 8](#). As previously mentioned, it signifies both the convergence and diversity of solutions. It is considered that the higher the indicator value, the better the quality of

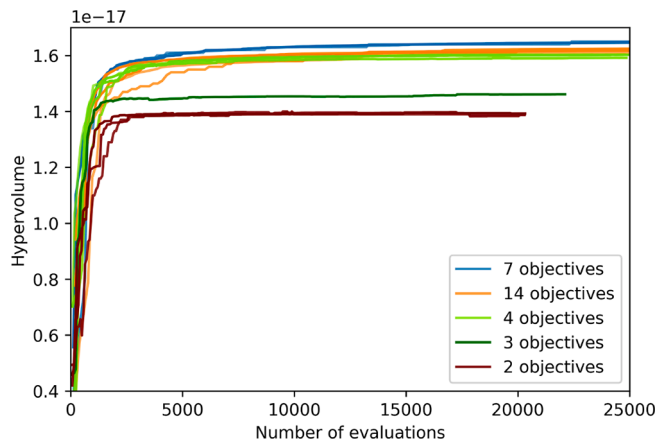


Fig. 8. Hypervolume indicator for different simulation runs.

the solutions. It is calculated for the Pareto solutions obtained after each generation for each simulation run. As outlined, it was calculated for all 14 objectives, even if objectives were temporarily omitted during the optimization. The anti-ideal point for the indicator calculation corresponds to approximately 30% worse objective values than the maximum obtained in the preliminary simulation runs.

It can be seen that for all five runs, optimizing with the reduced seven objectives has a better quality of solutions than the original 14 objectives. This can be seen with the higher hypervolume indicator for the former case. Optimizing with 14 indicators struggled to reach a similar hypervolume value, even for the same amount of generations or more than twice the number of evaluations (see figures S1 and S2 in supplementary material).

As the indicators were reduced beyond seven, the solution quality or

the hypervolume was also reduced. The hypervolume indicator with four indicators is almost the same as or slightly less than with the 14 objectives. For further reduction in indicators, the hypervolume indicator value was considerably less.

It should be noted that the comparison of hypervolume is fair with respect to the number of evaluations since the number of evaluations for each generation differs depending on the number of objectives optimized (see Table 1). For example, optimization with 14 objectives requires approximately two times more function evaluations than with seven objectives, due to having twice the population size. In any case, the above observations do not change even when a comparison is made with respect to the number of generations.

4.2. 2D plots of the Pareto front

In this section, we take a look closer at the Pareto solutions obtained to draw further insights into their quality. The Pareto solutions provided by the different simulation runs are plotted on four bi-dimensional graphs. These are all Pareto-optimal solutions in the 'n' objective space. Where 'n' depends on the number of objectives (four, seven, and 14), it can be seen in the graph legends. These Pareto solutions were plotted for all 14 objectives in bi-dimensional plots at the end of 300 generations, but only four graphs are presented here. The number of individuals in the Pareto here is 3615, 8781, and 9951, for four, seven, and 14 objectives, respectively.

In Fig. 9, the Pareto solutions obtained by one simulation run of 14 and seven objectives can be seen, while in Fig. 10, a comparison is made between four and seven objective runs. An optimization with two objectives will give a single curve of points. Here, since the solutions optimal in higher dimensions are plotted in two dimensions, the Pareto curves are thicker. The same reason also explains the different shapes of these curves as compared to a 2-dimensional Pareto curve.

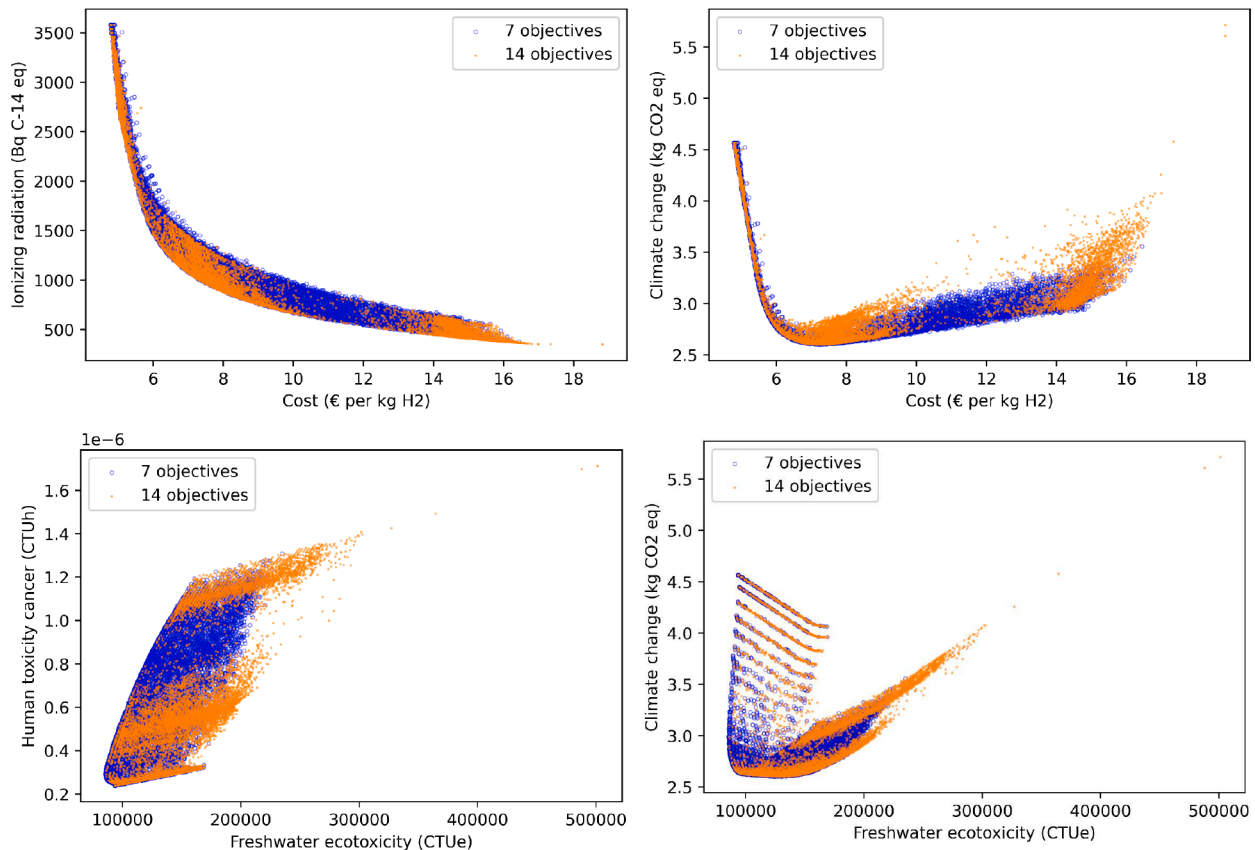


Fig. 9. Distribution of the Pareto front obtained using 14 and seven objectives shown in four figures of 2-dimensional plots.

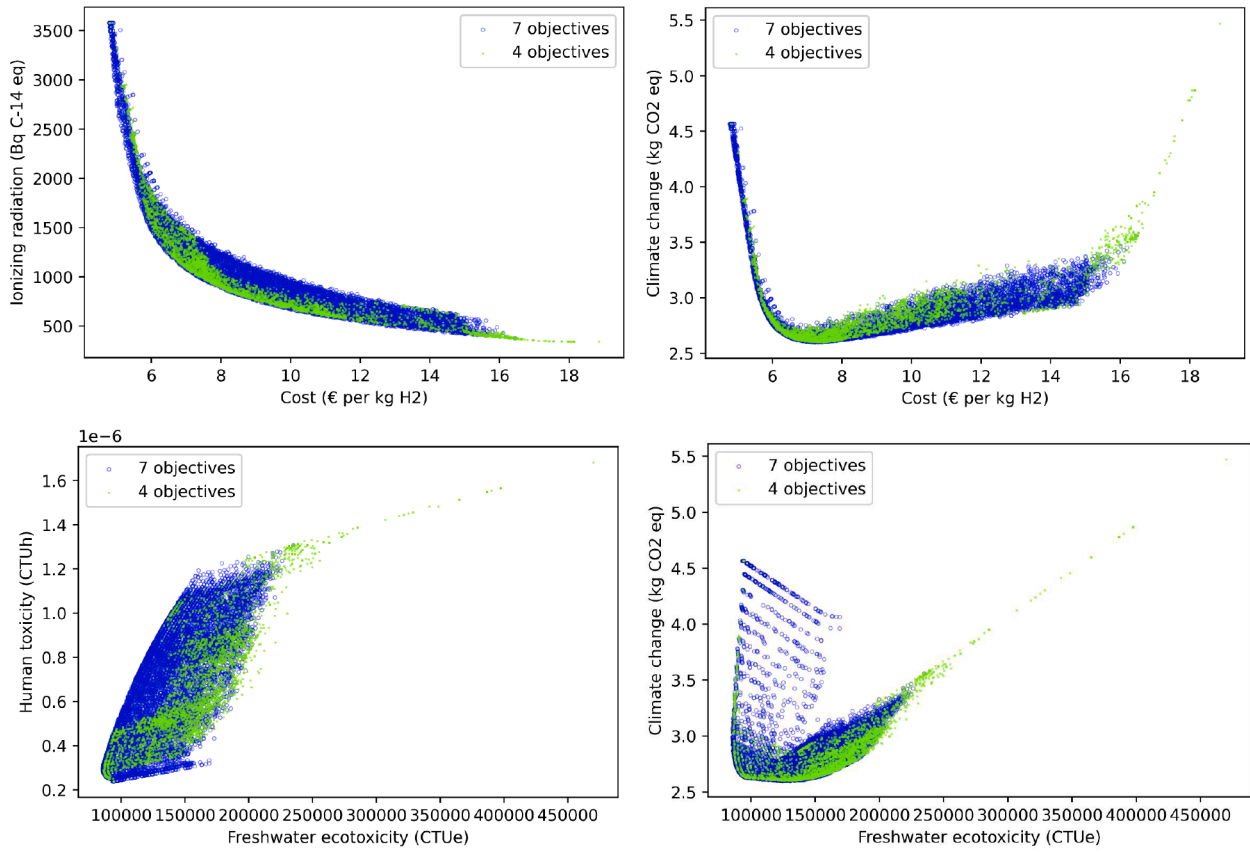


Fig. 10. The distribution of the Pareto front obtained using seven and four objectives shown in four figures of 2-dimensional plots.

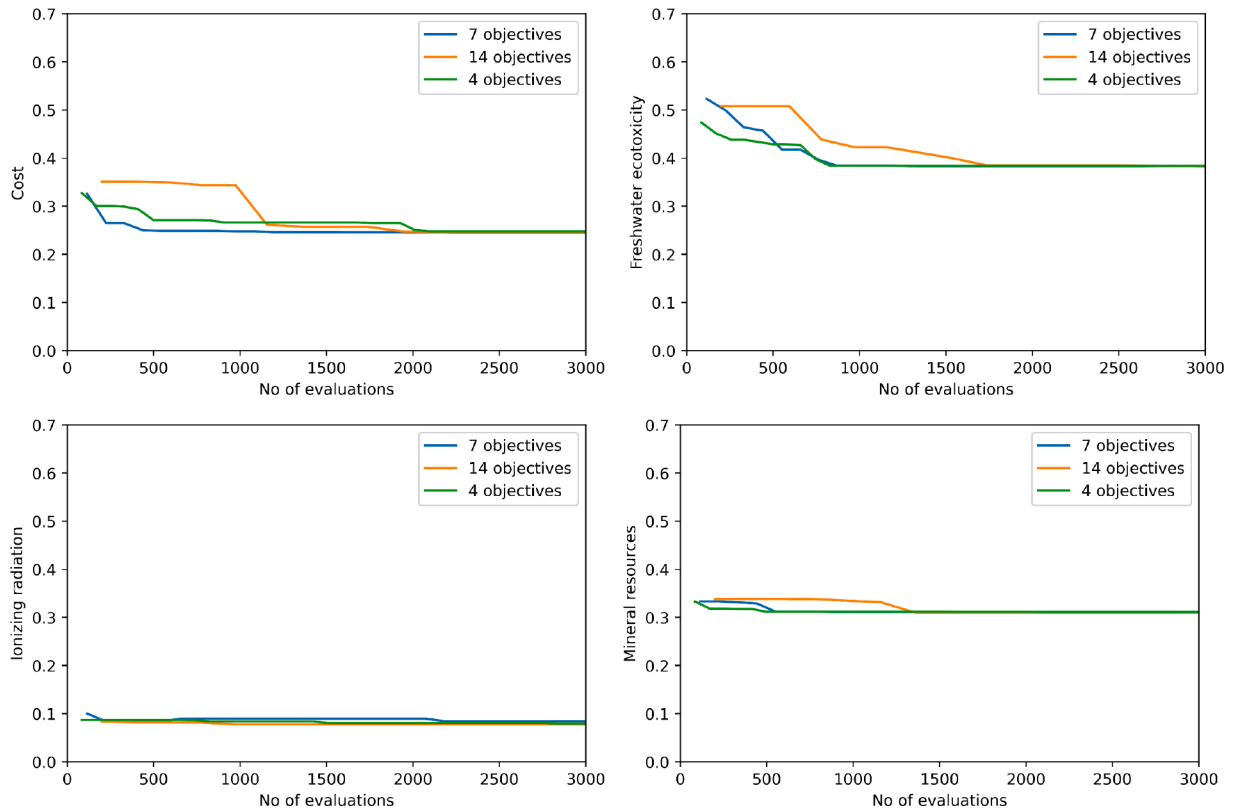


Fig. 11. The standardized minimum value of objectives versus the number of evaluations for different simulation runs.

Table 2

Estimation of computational time using many-processing for the different number of objectives.

	NSGA-III with 14 objectives	NSGA-III with reduction to 7 objectives	NSGA-III with reduction to 4 objectives	NSGA-III with reduction to 2 objectives
Time required for 200 generations on 8 cores (Intel i7, 7 th gen)	13 hours	7.5 hours	5.8 hours	5 hours
Quality of solutions	++	+++	++	+

In both Figures, the superior distribution of solutions obtained with seven objectives can be seen. Hence, it also validates the higher hypervolume indicator obtained for this instance. The comparatively worse distribution obtained with 14 objectives (with noticeable empty spaces in the plots) is likely due to the less distributed reference points in NSGA-III. To limit the size of the population and consequently the number of evaluations, a layering approach was used to specify reference points. As mentioned, a population for the next generation amongst the non-dominated members is selected after assigning each individual to a reference point. Then, the Pareto front is updated using this population if it is non-dominated compared to the individuals already present. Thus, it is likely that, due to insufficiently distributed reference points, the spread of solutions obtained also follows a similar trend. It should be noted that the optimization with 14 objectives has a higher number of evaluations and a higher number of Pareto-optimal points. Irrespective of this, it struggles to uniformly distribute the points, as can be seen in Fig. 9. Despite having a high number of points, they leave a noticeable space in the plots.

To analyze the importance of having a good distribution in many-objective optimization, consider the ionizing radiation versus cost plot in Fig. 9. Hypothetically, if optimization was made with respect to 14 objectives, and a practitioner wants to propose a solution with ionizing radiation around 1000 Bq C-14 eq and cost between €10-€12, they cannot, since there are not many orange points in that region.

For optimization with seven objectives, despite the lower number of Pareto-optimal points, they seem to be better distributed. Here too, a layering approach was used for reference point distribution. The number of reference points is decreased to half as compared to the original search space, but they are better distributed in the reduced seven objective space. Thus, better-distributed solutions in the reduced space could be found. Furthermore, since the seven objectives considered were highly correlated with the rest of the seven temporarily omitted objectives, the search provides a better distribution of solutions in all objectives.

On the other hand, the worse quality of solutions obtained with four objectives, as compared to seven objectives, is likely due to the 3% variance left out. The four objectives correspond to two PC retention, and in the PCA reduction procedure that explains 97% of the cumulative variance. As a result, 3% of the variance of the original objective space is not explained in this instance. Thus, solutions optimal in the higher dimensional space might have been discarded when optimizing with four objectives. The inferior performance is likely due to this reason, even though they have a high distribution of reference points.

The optimization instance with two reduced objectives obtained from PCA resulted in the worst performance. This was expected due to its low hypervolume indicator value. The most probable reason is that two objectives fail to capture the variance of the original problem, thus distorting the Pareto front. The 2-dimensional plots for two and seven objectives can be found in Figure S3 in the supplementary material. All of the observations seen above regarding the distribution of points are

the same for the multiple optimization runs.

4.3. Evaluations to reach a minimum value of indicators

In terms of searching the minimum value of each objective, these values were found relatively quickly for all instances with (seven and four) objectives being slightly faster. The minimum value of indicators in the Pareto was about the same for all simulation runs, except for the two objective cases. A comparatively lower value for some indicators, such as cost, was not reached, even after 300 generations for this instance.

A standardized minimum value of Pareto solutions for four objectives, plotted for the number of evaluations, is illustrated in Fig. 11. The minimum value of the objectives is standardized by dividing by the anti-ideal point used for hypervolume. Such standardization is important since LCA indicators show a difference in magnitude of up to 10^{12} between them. Thus, a small difference in indicators with high magnitude may seem significant and vice versa.

Since the performance of the two objective cases was considerably worse, and to ease the visualization, it is not plotted here. However, the same figures including it can be found in Figure S4 in the supplementary material.

In most indicators, such as cost, freshwater ecotoxicity, and mineral resource depletion, fewer objectives lead to a relatively faster search of the minimum objective value, while in others, such as ionizing radiations, no difference is found. However, it should be noted that finding minimum points might not reflect optimal solutions or a satisfactory distribution of Pareto points for decision-making. For all simulation runs, there was a negligible change in the hypervolume and the indicators after around 200 generations, hence the simulations were run for a maximum of 300 generations each.

5. Discussion

5.1. Objective reduction using PCA

The important observation to highlight here is objective reduction after a certain point might significantly distort the original Pareto front. The CUT value of 99.99% without additional reduction in the last step (see Fig. 5) gave the best quality solutions in terms of convergence and diversity. This adds new information to the proposed framework from Saxena et al. [33]. They recommend a low CUT value, and additional reduction using a correlation matrix is recommended for problems with a high number of redundant indicators. Since LCA indicators are also highly correlated, these steps were followed, and only two indicators were retained.

However, out of all of the simulation runs, the worst quality solutions were obtained in this case ($1,t$ instance). Considerably better solution quality in terms of convergence and diversity is obtained with three, four, and seven objectives. While it might be true that two indicators explain the majority of the variance, a small amount of variance left out in the indicators resulted in much worse solutions. Thus, objective reduction after a certain point might significantly distort the original Pareto front.

The other observation is that LCA can indeed be considered a problem with a high number of redundant indicators, meaning that the number of reduced objectives explaining most of the variance is much smaller than the original objective set. This was also observed in other investigations [26,32,51].

5.2. Performance of NSGA-III

It was found that NSGA-III struggles to provide a uniform distribution of solutions with 14 objectives, even though its capabilities have been demonstrated in other investigations in the literature with an equivalent or higher number of objectives. It shows that the

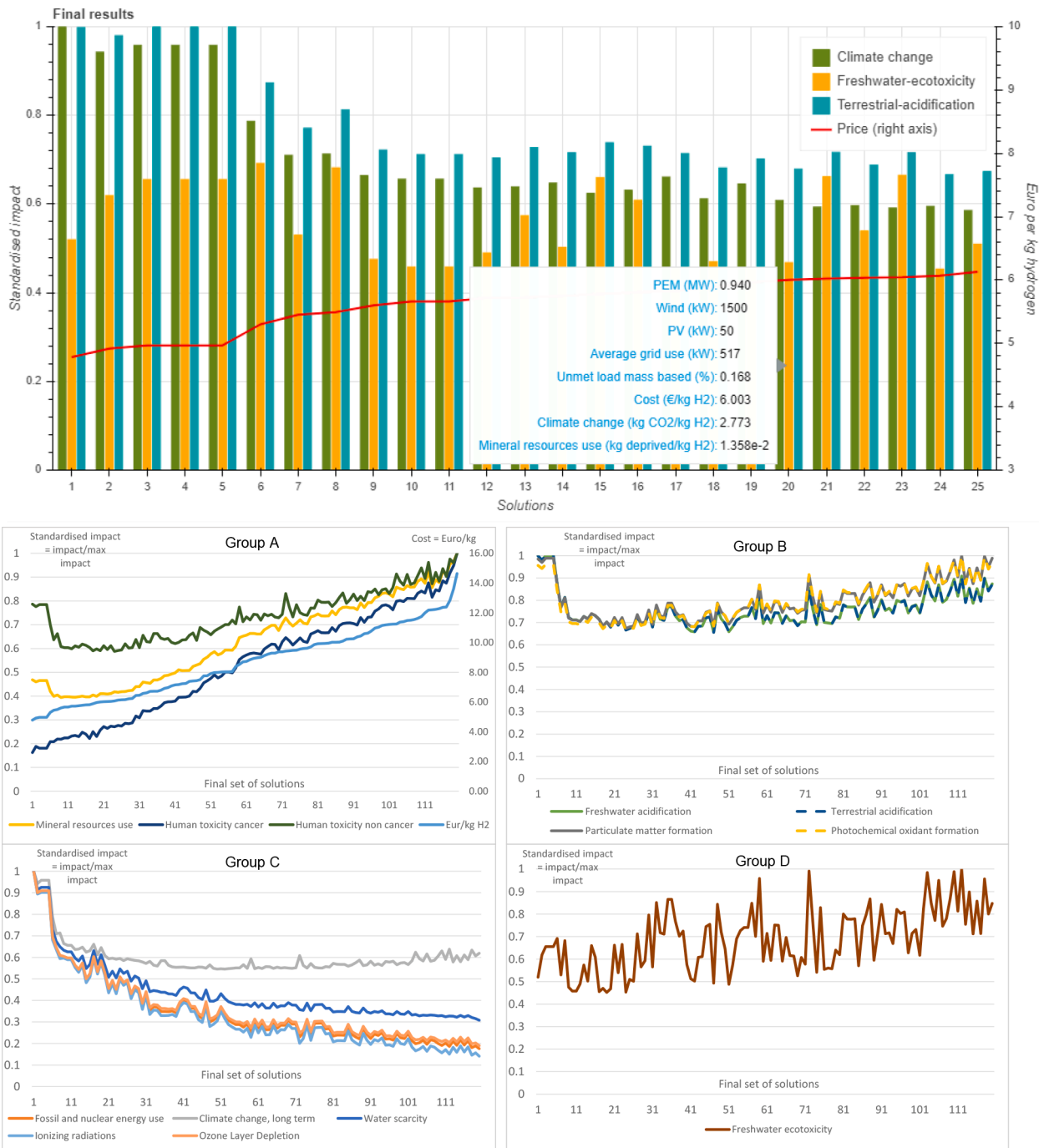


Fig. 12. Visualization of selected Pareto-optimal solutions. Above there are 25 arbitrary selected pareto optimal solutions with four indicators. The correlations of rest of the 10 indicators are shown below.

performance of algorithms is problem-dependent, which was also highlighted in the literature [23]. Nevertheless, NSGA-III performed well with most problems, and no one algorithm has the best performance with all types of problems (ibid.). The issue here is likely due to the inadequate distribution of the reference points due to the high number of objectives. The number of reference points could be increased, but it will lead to an exponential increase in computational time. For example, increasing axis partitions from [2,2] to [3,2] in Table 1 leads to 665 reference points for 14 objectives. This will result in three times the computational time.

5.3. Performance of NSGA-III with reduced objectives

The best quality solutions were found when NSGA-III was run with the seven reduced objectives. This was verified using the hypervolume indicator values and the distribution of Pareto-optimal points. The probable reason behind this is the best trade-off was obtained between a good distribution of the supplied reference points to NSGA-III, and enough indicators retained to explain the variance of the original 14 objective problems.

If the objectives were reduced further, a corresponding decrease in the quality of solutions was noticed. For optimization with less than seven objectives, a lower hypervolume indicator was obtained than for the ones found with the original 14 objective optimizations. The worst

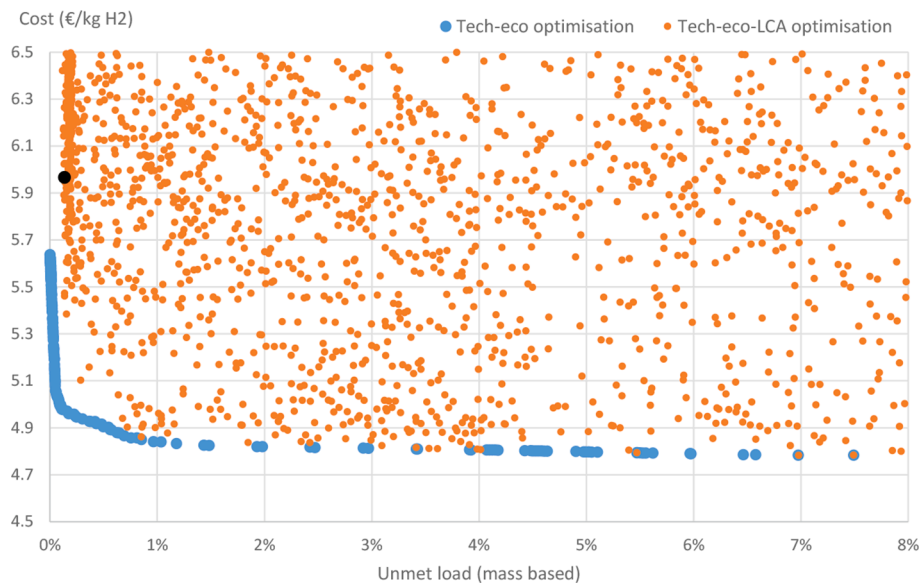


Fig. 13. Comparison of tech-eco optimization and with LCA. The black point is solution number 20 in Fig. 12.

solution quality was obtained when the problem was simplified to two objectives.

5.4. Time comparison

As mentioned before, hybrid energy simulations are computationally expensive. For this case, one simulation takes around nine seconds to complete on one core. The majority of the time is used by the energy simulation model (≈ 8 s) while the LCA model on Brightway2 takes the rest (≈ 1 s). The latter can be further reduced using aggregated pre-samples [52]. Estimation of the time required is made in Table 2, using the population size calculated in Table 1 as the approximate number of evaluations in each generation. The time required to generate samples at five generations of 14 objectives is not included for reduced objectives. The quality of the obtained solutions above is qualitatively rated.

Objectives when reduced to seven in the case study give the best quality solutions overall and in less time than the 14 objectives. If objectives are reduced further, a trade-off between the time required and the solution quality could be seen. The time required can be further reduced using more processing power by utilizing other computers on the network. This is often done both in our laboratory and in the literature.

5.5. Visualization

The solutions of interest from the Pareto front can be selected using the bi-dimensional plot or filtered using indicator values (e.g. < 3 CO₂-eq/kg H₂). For visualization, one of the optimization runs with seven objectives is selected, since the best quality of solutions were obtained in these runs. The objectives are standardized with respect to the maximum value and grouped according to their correlations. Correlated objectives can be seen below in Fig. 12, while above there are 25 arbitrarily selected Pareto-optimal solutions, such that only one indicator from each group below is displayed (when the mouse hovers over the tool, additional information about each solution is displayed). It can be observed that the high correlations between the indicators can also help in the visualization of the solutions. A practitioner can thus base their decision on limited indicators while having an overview of all the other indicators.

5.6. Comparison with techno-economic optimization

A comparison between the Pareto solutions for seven objective search (orange points) is made with two objective techno-economic search (blue points) in Fig. 13. As expected, it can be seen that not all solutions that are optimal in the techno-economic-LCA objectives are Pareto-optimal in the 2-dimensional techno-economic plane. As a result, in the status quo when a search is made with only two objectives, and the system is sized for techno-economic objectives, it is not possible to search for solutions with higher environmental efficiency. For example, all the blue points have a climate change indicator of approx 4.6 kg CO₂-eq/kg H₂. The maximum sizing of wind and PV is 0 and 50 kW respectively. If, for instance, climate change impact is desired to be decreased, arbitrary sizing of wind or PV has to be manually done. In this case, non-optimal solutions will likely be obtained, whereas, for Pareto-optimal solutions, an objective value can only be improved if at least one of the other objectives is made worse.

Theoretically, all the blue points should also be a part of the orange points in the Figure above. Some overlap at the bottom can be seen already. This can be improved in the future by modifying the reference points.

6. Conclusions

This paper explored an approach to take into account a high number of LCA indicators to avoid impact transfer during the many-objective search for Pareto optimal solutions for energy systems. For this purpose, the genetic algorithm NSGA-III was combined with PCA-based objective reduction which gives important observations for its use.

With the original 14 indicators, NSGA-III struggled to provide a uniform distribution of Pareto-optimal solutions. The objective reduction did improve the performance of the optimization search in terms of both: the quality of solutions and computational time. However, it was also found that a reduction in objectives beyond a certain point led to a reduction in computational time but also a deterioration in the quality of Pareto solutions obtained. The best quality solutions were obtained when the original 14 indicators were reduced to seven. This corresponds to the following setting in the PCA reduction framework: CUT value maintained at 99.99% without additional reduction using a correlation matrix.

More research is needed to determine whether the same settings in the PCA framework also give better solution quality for other problems.

Nonetheless, the important conclusion here is against the use of recommended settings in the framework of Saxena et al., as it might oversimplify and significantly distort the original Pareto front [33].

CRedit authorship contribution statement

Hemant Sharma: Conceptualization, Methodology, Investigation, Software, Writing - original draft. **Guillaume Mandil:** Validation, Resources, Data curation, Writing - review & editing, Supervision. **Élise Monnier:** Validation, Resources, Data curation, Writing - review & editing, Supervision. **Emmanuelle Cor:** Validation, Resources, Data curation, Writing - review & editing, Supervision. **Peggy Zwolinski:** Validation, Resources, Data curation, Writing - review & editing, Supervision.

Declaration of Competing Interest

The authors declare that they have no known competing financial interests or personal relationships that could have appeared to influence the work reported in this paper.

Data availability

Data will be made available on request.

Appendix A. Supplementary data

Supplementary data associated with this article can be found, in the online version, at <https://doi.org/10.1016/j.ecmx.2023.100361>.

References

- Pachauri R, Meyer L, Climate change 2014: Synthesis report. contribution of working groups i, ii and iii to the fifth assessment report of the intergovernmental panel on climate change.
- Al-Falahi MD, Jayasinghe S, Enshaei H. A review on recent size optimization methodologies for standalone solar and wind hybrid renewable energy system. *Energy Conversion Manage* 2017;143:252–74.
- Sharma H, Monnier E, Mandil G, Zwolinski P, Colasson S. Comparison of environmental assessment methodology in hybrid energy system simulation software. *Procedia CIRP* 2019;80:221–7. <https://doi.org/10.1016/j.procir.2019.01.007>. URL: <https://linkinghub.elsevier.com/retrieve/pii/S2212827119300095>.
- Turconi R, Boldrin A, Astrup T. Life cycle assessment (lca) of electricity generation technologies: Overview, comparability and limitations. *Renew Sustainable Energy Rev* 2013;28:555–65.
- Azapagic A, Clift R. Life cycle assessment and multiobjective optimisation. *J Cleaner Prod* 1999;7(2):135–43.
- Zhang D, Evangelisti S, Lettieri P, Papageorgiou LG. Optimal design of chp-based microgrids: Multiobjective optimisation and life cycle assessment. *Energy* 2015;85:181–93.
- Yue D, Pandya S, You F. Integrating hybrid life cycle assessment with multiobjective optimization: a modeling framework. *Environ Sci Technol* 2016;50(3):1501–9.
- Antipova E, Boer D, Guillén-Gosálbez G, Cabeza LF, Jiménez L. Multi-objective optimization coupled with life cycle assessment for retrofitting buildings. *Energy Build* 2014;48:92–9.
- Vandepaer L, Panos E, Bauer C, Amor B. Energy system pathways with low environmental impacts and limited costs: Minimizing climate change impacts produces environmental cobenefits and challenges in toxicity and metal depletion categories. *Environ Sci Technol* 2020;54(8):5081–92.
- Gerber L, Gassner M, Maréchal F. Systematic integration of LCA in process systems design: Application to combined fuel and electricity production from lignocellulosic biomass. *Comput Chem Eng* 2011;35(7):1265–80. <https://doi.org/10.1016/j.compchemeng.2010.11.012>. URL: <https://linkinghub.elsevier.com/retrieve/pii/S0098135410003595>.
- Ahmadi A, Tiruta-Barna L. A process modelling-life cycle assessment-multiobjective optimization tool for the eco-design of conventional treatment processes of potable water. *J Cleaner Prod* 2015;100:116–25.
- Nagapurkar P, Smith JD. Techno-economic optimization and environmental life cycle assessment (lca) of microgrids located in the us using genetic algorithm. *Energy Convers Manage* 2019;181:272–91.
- Luo Z, Yang S, Xie N, Xie W, Liu J, Agbodjan YS, Liu Z. Multi-objective capacity optimization of a distributed energy system considering economy, environment and energy. *Energy Convers Manage* 2019;200:112081.
- Dietz A, Azzaro-Pantel C, Pibouleau L, Domenech S. Multiobjective optimization for multiproduct batch plant design under economic and environmental considerations. *Comput Chem Eng* 2006;30(4):599–613.
- Antipova E, Boer D, Cabeza LF, Guillén-Gosálbez G, Jiménez L. Uncovering relationships between environmental metrics in the multi-objective optimization of energy systems: A case study of a thermal solar rankine reverse osmosis desalination plant. *Energy* 2013;51:50–60.
- Huijbregts M, Steinmann Z, Elshout P, Stam G, Verones F, Vieira M, et al., Recipe 2016: a harmonized life cycle impact assessment method at midpoint and endpoint level report i: characterization.
- Bulle C, Margni M, Patouillard L, Boulay A-M, Bourgault G, De Bruille V, Cao V, Hauschild M, Henderson A, Humbert S, Kashef-Haghghi S, Kounina A, Laurent A, Levasseur A, Liard G, Rosenbaum RK, Roy P-O, Shaked S, Fantke P, Jolliet O. IMPACT World+: A globally regionalized life cycle impact assessment method. *Int J Life Cycle Assess* 2019;24(9):1653–74. <https://doi.org/10.1007/s11367-019-01583-0>. URL: <http://link.springer.com/10.1007/s11367-019-01583-0>.
- Baghaee HR, Mirsalim M, Gharehpetian GB. Multi-objective optimal power management and sizing of a reliable wind/pv microgrid with hydrogen energy storage using mopso. *Journal of Intelligent & Fuzzy Systems* 2017;32(3):1753–73.
- V.O. Okinda, N.O. Abungu, A review of techniques in optimal sizing of hybrid renewable energy systems.
- Hassan R, Cohanin B, De Weck O, Venter G. A comparison of particle swarm optimization and the genetic algorithm. In: 46th AIAA/ASME/ASCE/AHS/ASC structures, structural dynamics and materials conference; 2005. p. 1897.
- Panda S, Padhy NP. Comparison of particle swarm optimization and genetic algorithm for facts-based controller design. *Appl Soft Comput* 2008;8(4):1418–27.
- Marler RT, Arora JS. Survey of multi-objective optimization methods for engineering. *Struct Multidisciplinary Optimization* 2004;26(6):369–95.
- Li K, Wang R, Zhang T, Ishibuchi H. Evolutionary many-objective optimization: A comparative study of the state-of-the-art. *IEEE Access* 2018;6:26194–214.
- Deb K, Jain H. An evolutionary many-objective optimization algorithm using reference-point-based nondominated sorting approach, part i: solving problems with box constraints. *IEEE Trans Evol Comput* 2013;18(4):577–601.
- Jain H, Deb K. An evolutionary many-objective optimization algorithm using reference-point based nondominated sorting approach, part ii: handling constraints and extending to an adaptive approach. *IEEE Trans Evol Comput* 2013;18(4):602–22.
- Steinmann ZJ, Schipper AM, Hauck M, Huijbregts MA. How many environmental impact indicators are needed in the evaluation of product life cycles? *Environ Sci Technol* 2016;50(7):3913–9.
- Perez-Gallardo JR, Azzaro-Pantel C, Astier S. Combining multi-objective optimization, principal component analysis and multiple criteria decision making for ecodesign of photovoltaic grid-connected systems. *Sustainable Energy Technol Assess* 2018;27:94–101.
- Yuan Y, Ong Y-S, Gupta A, Xu H. Objective reduction in many-objective optimization: evolutionary multiobjective approaches and comprehensive analysis. *IEEE Trans Evol Comput* 2017;22(2):189–210.
- Brockhoff D, Zitzler E. Improving hypervolume-based multiobjective evolutionary algorithms by using objective reduction methods. In: 2007 IEEE congress on evolutionary computation. IEEE; 2007. p. 2086–93.
- Gonzalez-Garay A, Guillen-Gosalbez G. Suscape: A framework for the optimal design of sustainable chemical processes incorporating data envelopment analysis. *Chem Eng Res Des* 2018;137:246–64.
- Deb K, Saxena DK. On finding pareto-optimal solutions through dimensionality reduction for certain large-dimensional multi-objective optimization problems, *Kangal report* 2005011.
- Perez Gallardo JR, Ecodesign of large-scale photovoltaic (pv) systems with multi-objective optimization and life-cycle assessment (lca), Ph.D. thesis (2013).
- Saxena DK, Duro JA, Tiwari A, Deb K, Zhang Q. Objective reduction in many-objective optimization: Linear and nonlinear algorithms. *IEEE Trans Evol Comput* 2012;17(1):77–99.
- Mutel C. Brightway: An open source framework for Life Cycle Assessment. *JOSS* 2017;2(12):236. <https://doi.org/10.21105/joss.00236>. URL: <http://joss.theoj.org/papers/10.21105/joss.00236>.
- Guinot B, Bultel Y, Montignac F, Riu D, Pinton E, Noiro-Le Borgne I. Economic impact of performances degradation on the competitiveness of energy storage technologies – Part 1: Introduction to the simulation-optimization platform ODYSSEY and elements of validation on a PV-hydrogen hybrid system. *Int J Hydrog Energy* 2013;38(35):15219–32. <https://doi.org/10.1016/j.ijhydene.2013.08.125>. URL: <https://linkinghub.elsevier.com/retrieve/pii/S0360319913021356>.
- Bareiß K, de la Rua C, Möckl M, Hamacher T. Life cycle assessment of hydrogen from proton exchange membrane water electrolysis in future energy systems. *Appl Energy* 2019;237:862–72. <https://doi.org/10.1016/j.apenergy.2019.01.001>. URL: <https://linkinghub.elsevier.com/retrieve/pii/S03606261919300017>.
- Zhao G, Ravn Nielsen E. Environmental Impact Study of BIG HIT, Department of Energy Conversion and Storage. Technical University of Denmark 2018. <https://orbit.dtu.dk/en/publications/environmental-impact-study-of-big-hit>.
- Pfenninger S, Staffell I. Long-term patterns of european pv output using 30 years of validated hourly reanalysis and satellite data. *Energy* 2016;114:1251–65. <https://doi.org/10.1016/j.energy.2016.08.060>. URL: <https://www.renewables.ninja/>.
- Gazbour N, Razongles G, Schaeffer C, Charbuillet C. Photovoltaic power goes green. In: 2016 Electronics Goes Green 2016+(EGG). IEEE; 2016. p. 1–8.
- Staffell I, Pfenninger S. Using bias-corrected reanalysis to simulate current and future wind power output. *Energy* 2016;114:1224–39. <https://doi.org/10.1016/j.energy.2016.08.068>. URL: <https://www.renewables.ninja/>.

- [41] Sacchi R, Besseau R, Pérez-López P, Blanc I. Exploring technologically, temporally and geographically-sensitive life cycle inventories for wind turbines: A parameterized model for denmark. *Renewable Energy* 2019;132:1238–50. URL: https://github.com/romainsacchi/LCA_WIND_DK/blob/master/LCA_parameterized_model_Eolien_public.ipynb.
- [42] Padey P, Girard R, Le Boulch D, Blanc I. From lcas to simplified models: a generic methodology applied to wind power electricity. *Environ Sci Technol* 2013;47(3):1231–8.
- [43] Wernet G, Bauer C, Steubing B, Reinhard J, Moreno-Ruiz E, Weidema B. The ecoinvent database version 3 (part I): Overview and methodology. *Int J Life Cycle Assess* 2016;21(9):1218–30. <https://doi.org/10.1007/s11367-016-1087-8>. URL: <http://link.springer.com/10.1007/s11367-016-1087-8>.
- [44] Fortin F-A, De Rainville F-M, Gardner M-AG, Parizeau M, Gagné C. Deap: Evolutionary algorithms made easy. *J Mach Learn Res* 2012;13(1):2171–5.
- [45] Das I, Dennis JE. Normal-boundary intersection: A new method for generating the pareto surface in nonlinear multicriteria optimization problems. *SIAM J Optim* 1998;8(3):631–57.
- [46] Pozo C, Ruiz-Femenia R, Caballero J, Guillén-Gosálbez G, Jiménez L. On the use of principal component analysis for reducing the number of environmental objectives in multi-objective optimization: Application to the design of chemical supply chains. *Chem Eng Sci* 2012;69(1):146–58.
- [47] Bechikh S, Datta R, Gupta A. Recent advances in evolutionary multi-objective optimization, Vol. 20. Springer; 2016.
- [48] While L, Bradstreet L, Barone L. A fast way of calculating exact hypervolumes. *IEEE Trans Evol Comput* 2011;16(1):86–95. URL: <https://pypi.org/project/hvwfg/>.
- [49] Ishibuchi H, Imada R, Setoguchi Y, Nojima Y. How to specify a reference point in hypervolume calculation for fair performance comparison. *Evol Comput* 2018;26(3):411–40.
- [50] Zitzler E, Thiele L, Laumanns M, Fonseca CM, Da Fonseca VG. Performance assessment of multiobjective optimizers: An analysis and review. *IEEE Trans Evol Comput* 2003;7(2):117–32.
- [51] Sabio N, Kostin A, Guillén-Gosálbez G, Jiménez L. Holistic minimization of the life cycle environmental impact of hydrogen infrastructures using multi-objective optimization and principal component analysis. *Int J Hydrog Energy* 2012;37(6):5385–405. <https://doi.org/10.1016/j.ijhydene.2011.09.039>. URL: <https://linkinghub.elsevier.com/retrieve/pii/S0360319911021501>.
- [52] Lesage P, Mutel C, Schenker U, Margni M. Uncertainty analysis in lca using precalculated aggregated datasets. *Int J Life Cycle Assess* 2018;23(11):2248–65. URL: <https://bw2preagg.readthedocs.io/en/latest/>.